Biosensors and Bioelectronics 187 (2021) 113292

Contents lists available at ScienceDirect

Biosensors and Bioelectronics

journal homepage: www.elsevier.com/locate/bios

G-triplex: A new type of CRISPR-Cas12a reporter enabling highly sensitive nucleic acid detection

Tao Li [a,b,1], Rui Hu [a,b,1], Jianbo Xia [c,1], Zhichen Xu [a,b], Dongjuan Chen [c], Jinou Xi [c], Bi-Feng Liu [d], Jiang Zhu [a,b], Ying Li [a,b,*], Yunhuang Yang [a,b], Maili Liu [a,b,**]

[a] State Key Laboratory of Magnetic Resonance and Atomic Molecular Physics, Wuhan National Laboratory for Optoelectronics, National Centre for Magnetic Resonance in Wuhan, Wuhan Institute of Physics and Mathematics, Innovation Academy for Precision Measurement Science and Technology, Chinese Academy of Sciences - Wuhan National Laboratory for Optoelectronics, Huazhong University of Science and Technology, Wuhan, 430071, China

[b] University of Chinese Academy of Sciences, Beijing, 10049, China

[c] Department of Laboratory Medicine, Maternal and Child Health Hospital of Hubei Province, Tongji Medical College, Huazhong University of Science and Technology, Wuhan, 430070, China

[d] The Key Laboratory for Biomedical Photonics of MOE at Wuhan National Laboratory for Optoelectronics - Hubei Bioinformatics & Molecular Imaging Key Laboratory, Systems Biology Theme, Department of Biomedical Engineering, College of Life Science and Technology, Huazhong University of Science and Technology, Wuhan, 430074, China

ARTICLE INFO

Keywords:
CRISPR-Cas12a
G-triplex
Biosensor
Trans-cleavage
Nucleic acid detection

ABSTRACT

CRISPR-Cas12a (Cpf1) trans-cleaves ssDNA and this feature has been widely harnessed for nucleic acid detection. Herein, we introduce a new type of Cas12a reporter, G-triplex (G3), and a highly sensitive biosensor termed G-CRISPR. We proved that Cas12a trans-cleaves G3 structures in about 10 min and G3 can serve as an excellent reporter based on the cleavage-induced high-order structure disruption. G3 reporter improves the analytical sensitivity up to 20 folds, enabling the detection of unamplified and amplified DNA as low as 50 pmol and 0.1 amol (one copy/reaction), respectively. G-CRISPR has been utilized for the analysis of 27 PCR-amplified patient samples with HPV infection risk based on both fluorescence and lateral flow assays, resulting in 100% concordance between the two. In comparison with the clinical results, it achieved overall specificity and sensitivity of 100% and 94.7%, respectively. These results suggest that G-CRISPR can serve as a rapid, sensitive, and reliable biosensor, and could further expand the CRISPR toolbox in biomedical diagnostics.

1. Introduction

CRISPR-Cas system serves as an adaptive immunity system in bacteria and archaea to protect them against invading phages, virus and plasmids (Barrangou et al., 2007; Doudna and Charpentier, 2014). During the interplay between pathogens and their hosts, CRISPR-Cas machinery cleaves specific DNA with the guide of CRISPR RNA (crRNA) (Koonin et al., 2017). This property has been harnessed by scientists to revolutionize gene editing with the emergence of many Cas proteins such as Cas9, Cas12, Cas13, and Cas14 (Abudayyeh et al., 2016; Harrington et al., 2018; Jinek et al., 2012; Pan et al., 2019; Zetsche et al., 2015). Recently, a growing body of research has demonstrated that certain Cas proteins exhibit collateral cleavage on non-specific targets (termed trans-cleavage) after the target-specific cleavage (termed cis-cleavage) (Abudayyeh et al., 2016; Gootenberg et al. 2017, 2018bib_Gootenberg_et_al_2018bib_Gootenberg_et_al_2017; Li et al., 2018a). Leveraging this special characteristic, numerous CRISPR-based point-of-care (POC) platforms (e.g., SHERLOCK) have been developed for human genotyping and pathogen detection, with high specificity and sensitivity (Fozouni et al., 2020; Gootenberg et al. 2017, 2018bib_Gootenberg_et_al_2018bib_Gootenberg_et_al_2017; Xiong et al., 2020a).

Among the CRISPR proteins, Cas12a (also known as Cpf1) (Zetsche et al., 2015) offers promiscuous endonuclease activities that trans-cleave non-target ssDNA (but not dsDNA and RNA) (Chen et al., 2018; Li et al.,

* Corresponding author. State Key Laboratory of Magnetic Resonance and Atomic Molecular Physics, Wuhan National Laboratory for Optoelectronics, National Centre for Magnetic Resonance in Wuhan, Wuhan Institute of Physics and Mathematics, Innovation Academy for Precision Measurement Science and Technology, Chinese Academy of Sciences - Wuhan National Laboratory for Optoelectronics, Huazhong University of Science and Technology, Wuhan, 430071, China.

** Corresponding author. University of Chinese Academy of Sciences, Beijing, 10049, China.

E-mail addresses: liying@wipm.ac.cn (Y. Li), ml.liu@wipm.ac.cn (M. Liu).

[1] These authors contributed equally to this work.

https://doi.org/10.1016/j.bios.2021.113292
Received 19 February 2021; Received in revised form 19 April 2021; Accepted 27 April 2021
Available online 9 May 2021

2018a; Swarts and Jinek, 2019). Using a ssDNA as the reporter, Chen et al. established the 'DETECTR' platform that achieved attomole (aM) sensitivity for human papillomavirus (HPV) detection (Chen et al., 2018). Li et al. implemented a similar ssDNA-FQ reporter and developed a system named 'HOLMES', and detected pseudorabies virus (RNA) and Japanese encephalitis virus (RNA) (Li et al., 2018b). Its sensitivity is around 10 aM for the detection of amplified targets. Thereafter, many other strategies have been proposed to optimize the performance of Cas12a-based platforms, such as to diversify the target types (e.g., combine aptamer to detect protein, small molecules besides DNA/RNA) (Dai et al., 2019; Liang et al., 2019; Xiong et al., 2020b; Yuan et al., 2020), to simplify the operation protocol (e.g., automatic sample extraction, one-pot detection) (Ding et al., 2020; Joung et al., 2020; Ramachandran et al., 2020), and to avoid the use of reader (Broughton et al., 2020; Shao et al., 2019; Wang et al., 2020b). Another key goal of the optimization is to improve the detection sensitivity, which could reduce the assay time without sacrificing accuracy during early viral infection (Jin et al., 2020; van Dongen et al., 2020; Wang et al., 2020a). For example, researchers have introduced two crRNAs (Ding et al., 2020) and replaced Mg^{2+} with Mn^{2+} to increase Cas12a activity (Ma et al., 2020), both of which realized detection sensitivity of a few copies of nucleic acids. However, to our knowledge, current Cas12-based detection systems commonly use ssDNA as the reporter, which represents a limitation to further improve the sensitivity.

Recently, we have reported that the activated CRISPR-Cas12a system trans-cleaves DNA G-quadruplexes (G4s) (Li et al., 2020). However, it requires a long time (up to several hours) to cleave G4 structures due to their high stability. G-triplex (G3), a DNA motif like G4, has three-stranded noncanonical secondary structure that can be formed by Guanine-rich DNA sequences through Hoogsteen-like hydrogen bonds (Cerofolini et al., 2014; Limongelli et al., 2013). G3 was initially recognized as an intermediate form of G4 with potentially important cellular functions (Koirala et al., 2012; Li et al., 2013), and further studies revealed that a few sequences could form stable G3 structures (Cerofolini et al., 2014; Koirala et al., 2012; Limongelli et al., 2013), though not as stable as G4s (Jiang et al., 2015). G3 shares multiple properties as G4 (e.g., sensitive to many stimuli such as metal ions, hemin, thioflavin T) (Demkovicova et al., 2017; Ida et al., 2019), thus it has emerged as a popular transducer of various types of biosensors (Wang et al., 2013; Zhao et al., 2019). For example, a G3 sequence, obtained by truncating four bases (GGGA) from a G4 sequence (Zhang et al., 2014), appeared to show strong affinity with methylene blue (MB) and could be stabilized by MB. This characteristic was utilized to develop an electrochemical biosensor for sensitive detection of cocaine (Zhao et al., 2019).

In this work, we showed that CRISPR-Cas12a could trans-cleave G3s and developed a sensitive nucleic acid detection platform based on this finding. We chose two typical G3 sequences, TBA11 (a truncated form of Thrombin Binding Aptamer or TBA) (Cerofolini et al., 2014; Limongelli et al., 2013) and telomere-G3 (Koirala et al., 2012) that were reported to be not so stable (Zhao et al., 2019), and investigated the cleavage activities of Cas12a on them. The results demonstrate that CRISPR-Cas12a trans-cleaves both G3 structures in a few minutes and the cleavage rate is much higher than that of G4. We verified this trans-cleavage activity with fluorescence spectroscopy, circular dichroism (CD) spectroscopy, gel electrophoresis, and nuclear magnetic resonance (NMR) experiments. Since G3 responds to various stimuli and can be degraded rapidly by the Cas12a system, it could be a promising reporter for building fast biosensors based on its high-order structural change before and after the cleavage. Accordingly, the G-CRISPR platform was developed by integrating CRISPR-Cas12a with the TBA11-G3 reporter. Using G-CRISPR, we successfully distinguished SARS-CoV-2 and SARS-CoV N-gene, and HPV16 and HPV18 L1-gene plasmids. The system achieved detection sensitivity of 50 pM and 0.1 aM (single copy per reaction) for the unamplified and amplified HPV16 plasmids respectively, improved up to 20 times over the ssDNA-reporter based Cas12a system. In addition, we demonstrated the successful detection of HPV16 and HPV18 in 27 patient samples using both fluorescent- and lateral flow-based G-CRISPR assays. The results are highly consistent with the clinical reports, resulting in a specificity and sensitivity of 100% and 94.7%, respectively. Overall, G-CRISPR offers high sensitivity and accuracy for nucleic acid detection and holds great potential to further expand the CRISPR-Cas12a toolbox for biosensing.

2. Experimental

2.1. Materials

G-triplex (G3), G-quadruplex (G4), and crRNA sequences were obtained from Sangon Biotech company (Shanghai, China). The SARS-CoV-2 N-gene, SARS-CoV N-gene, HPV16 L1-gene and HPV18 L1-gene were amplified via polymerase chain reaction (PCR) from pUC57-SARS-CoV-2-N, pUC57-SARS-CoV-N, pUC57-HPV16-L1 and pUC57-HPV18-L1 vector, respectively. PCR Master Mix was purchased from Yeasen company (ShangHai, China), and PCR products of the plasmids were purified by gel extraction kit (Axygen company, New York, American) before use. The primers and vectors used were synthesized by Tsingke company (Beijing, China). DNA and RNA sequences used were listed in Supporting Information (Table S1). DNA agarose and nucleic acid gel stain were purchased from Yeasen company (Shanghai, China). TEMED, $(NH_4)_2S_2O_8$, urea, 30% acrylamide/bis-acrylamide solution and 10 × TBE Buffer were purchased from Bio-Rad Laboratories (Hercules, CA). Lachnospiraceae bacterium ND2006 Cas12a (LbCas12a) was purchased from Magigen Biotech company (Guangzhou, China). Lateral flow strips (Milenia HybriDetect 1) were obtained from TwistDx (Cambridge, United Kingdom).

2.2. Cleavage assay

The protocol of cleavage assay was adapted from previous reports (Chen et al., 2018; Li et al., 2018a). Unless mentioned otherwise, Cas12a-based cleavage assays were carried out in the cleavage buffer consisting of 10 mM Tris, 70 mM KCl, 10 mM $MgCl_2$, pH 7.9. Prior to the assay, G3 and G4 oligonucleotides were heated at 95 °C for 10 min and cooled down before use. First, LbCas12a (1 μL, 2 μM), crRNA (2 μL, 1 μM) and cleavage buffer (17 μL) were mixed and preincubated at 37 °C for 10 min. After the formation of LbCas12a/crRNA complex, target DNA (5 μL, 100 nM) or non-target DNA (5 μL, 100 nM) or cleavage buffer (5 μL) and G3 or G4 oligonucleotides (25 μL, 500 nM) were added to form a 50-μL reaction solution. The cleavage reaction was performed at 37 °C for 15 min. To test the trans-cleavage activity of Cas12a on G3 and G4, SARS-CoV-2 or SARS-CoV N-gene plasmids were used (the relevant sequences are shown in Table S1). To test the specificity, sensitivity and limit-of-detection (LOD) of G-CRISPR, HPV16 and HPV18 plasmids were used. To detect the plasmid without preamplification, the target (HPV16, 100 nM) was diluted to 10 nM, 1 nM, 0.1 nM, 0.05 nM and 0.01 nM, respectively. To detect the plasmid with preamplification, the target (HPV16, 100 nM) was diluted to 10^{-13} M, 10^{-14} M, 10^{-15} M, 10^{-16} M, 10^{-17} M and 10^{-18} M respectively and amplified via PCR. The 50 μL PCR reaction solution consists of 2 × PCR Master Mix (25 μL), primer (2 × 2.5 μL, 10 μM), template DNA (10 μL) and ddH_2O (10 μL).

2.3. Measurement of fluorescence spectroscopy

Fluorescence spectroscopy can reveal the distance of the two fluorophores labelled at the two ends of the oligonucleotide, which can be used to evaluate the cleavage activities of Cas12a. To carry out the fluorescence assay, FRET (5′-FAM and 3′-TAMRA) or FQ (5′-FAM and 3′-BHQ1) labelled TBA11 or Telomere G3 sequences were diluted to a final concentration of 25 nM. Fluorescence measurements were performed on a FluoroMax-4 spectrofluorometer (Horiba, Japan) at room temperature (~25 °C). The excitation and emission slits were both 5 nm. Excitation

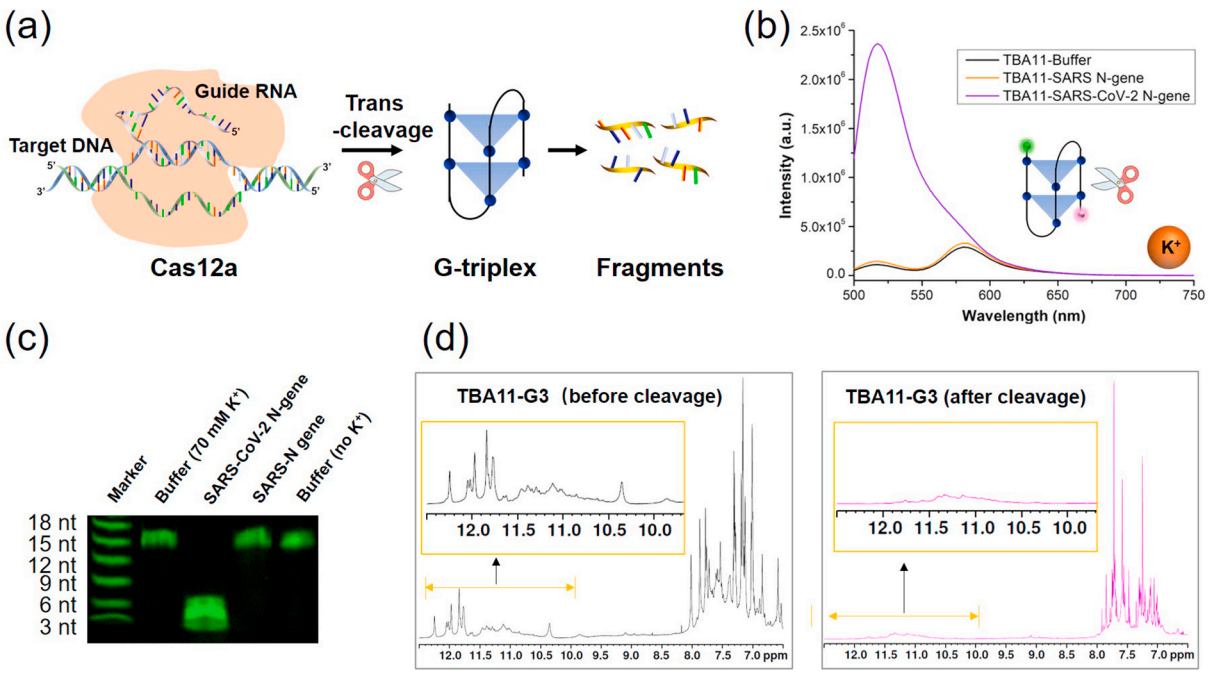

Fig. 1. ***The trans-cleavage of CRISPR-Cas12a on K^+ -induced TBA11-G3 structure.*** *(a) Scheme showing that the activated Cas12a system trans-cleaves the G-triplex structure into fragments. (b-d) Investigation of the trans cleavage by FRET (b), denaturing PAGE (c) and ^{1}H NMR (d). For lane 2 and lane 5 in (c), no plasmid was added.*

was set at 488 nm, and emission was collected from 500 to 750 nm. For quantitative analysis of the serial diluted HPV16 plasmid samples after PCR, the fluorescence value of these samples at 518 nm was corrected by subtracting the fluorescence value of background (without plasmid) at 518 nm.

For the time-course cleavage assay, the quartz cuvette holder was pre-heated and kept at 37 °C through a water circulation. LbCas12a (1 μL, 2 μM) was preincubated with crRNA (2 μL, 1 μM) at 37 °C for 10 min in a total of 20 μL cleavage buffer. Then FRET-labelled G3 or G4 sequences (50 μl, 5 μM) and 425 μL relevant buffer were mixed with 20 μL reaction solution. This mixture was added into the cuvette and incubated in the holder for another 10 min. After that, the measurement was initiated immediately after the target (5 μl, 100 nM) was added into the cuvette. The interval was set as 1–5 min based on the cleavage kinetics.

2.4. Circular dichroism (CD) experiment

Measurement of CD spectroscopy can provide the information whether the G3 structures are formed or degraded. CD experiments were carried out on Chirascan (Applied Photophysics, UK). The sample was put in a 0.1 cm path length cuvette and the data were collected by taking the average of three scans recorded from 220 to 320 nm at a scanning rate of 100 nm/min at room temperature (~25 °C). LbCas12a (1 μL, 2 μM) was preincubated with crRNA (2 μL, 1 μM) in a total of 20 μL relevant buffer (70 mM K^+ for TBA11, 100 mM Na^+ or 70 mM K^+ for telomere G3, respectively) for 10 min at 37 °C. Then the G3 oligonucleotide (25 μL, 25 μM) and the target (5 μL, 50 nM) were added into the reaction solution, followed by an incubation at 37 °C for 2 h. FRET assay was performed before the CD measurement to ensure that the G3 was fully cleaved. The mixture was diluted to a total volume of 250 μL for CD detection. All spectra were corrected with matched buffer blanks.

For the time-course CD measurement, the cuvette holder was pre-heated and kept at 37 °C, and the temperature of the testing solution was monitored with an on-stage sensor. LbCas12a (4 μL, 2 μM) was preincubated with crRNA (8 μL, 1 μM) in a total of 20 μL cleavage buffer (70 mM K^+) for 10 min at 37 °C. Then the TBA11 sequence (220 μl, 40 μM) and the target (10 μl, 100 nM) were mixed with the 20 μL reaction solution, followed by the CD measurement immediately with an interval of 10 min.

2.5. Denaturing PAGE

Denaturing polyacrylamide gel electrophoresis (PAGE) is able to resolve the cleaved elements with high resolution. Herein it was used to analyze the cleaved products of TBA11. LbCas12a (1 μL, 2 μM) was preincubated with crRNA (2 μL, 1 μM) in a total of 20 μL buffer (containing 70 mM K^+) for 10 min at 37 °C. Then FAM labelled TBA11 oligonucleotide (25 μL, 10 μM) and the target (5 μL, 50 nM) were added into the reaction solution and incubated at 37 °C for a predefined time period. The reaction solution was then incubated at 65 °C for 15 min to inactivate the LbCas12a. Next, the solution was mixed with the loading buffer and loaded into a 20% denaturing PAGE gel containing 8 M urea. Electrophoresis was performed at 120 V (about 40 V/cm) for about 90 min (Mini-PROTEAN Tetra Cell system, Bio-Rad) in 1 × TBE buffer. The gel was scanned using Bio-rad ChemiDoc MP (170–8280) (BioRad Company, Shanghai, China) in the mode of "fluorescein".

2.6. NMR experiments

NMR was used to characterize the construct of TBA11 and telomere G3. ^{1}H NMR spectra were measured on a Bruker AVANCE 700 MHz spectrometer at 10 °C. We dissolved TBA11 or telomere G3 (0.3 mM, without labelling fluorescent probes), LbCas12a (0.5 μM), and crRNA (0.5 μM) in 400 μL buffer composed of 90% H_2O/10% D_2O, 10 mM Tris (pH 7.9), 70 mM KCl (for TBA11) or 100 mM NaCl (for telomere G3), and 10 mM $MgCl_2$. NMR experiment was first performed on the non-cleaved sample. Then target DNA (15 nM, final concentration) was added to the sample and incubated at 37 °C for overnight cleavage. Structural change of the cleaved samples was assessed by CD spectroscopy before conducting NMR measurement to confirm full degradation. Then ^{1}H NMR spectrum was recorded on the cleaved sample with the same setting as the non-cleaved sample.

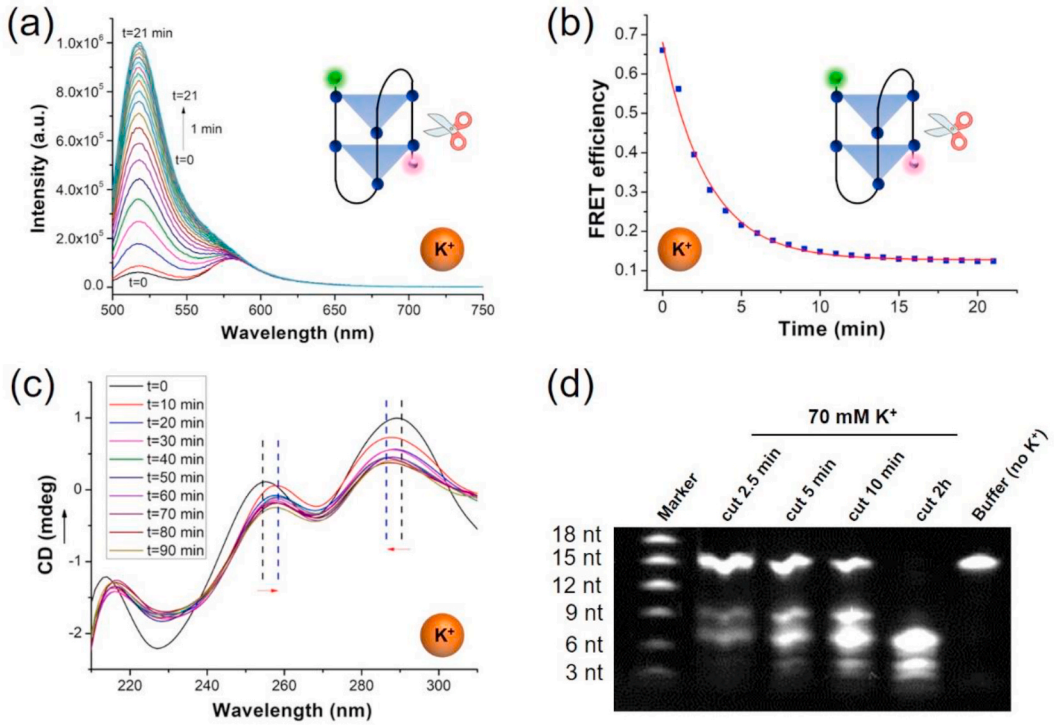

Fig. 2. Trans-cleavage kinetics of LbCas12a on 70 mM K^+ -induced TBA11. (a) Fluorescence spectra to show the time-course cleavage on TBA11. (b) FRET efficiency to show the cleavage kinetics. (c) CD spectra showing the time-course cleavage. (d) Products at different cleavage time points resolved by denaturing PAGE. For lane 6, no plasmid was added.

3. Results and discussion

3.1. Investigation of CRISPR-Cas12a trans-cleavage on TBA11-G3

G3 is a DNA motif that has similar secondary structure like G4. We hypothesized that G3 could be trans-cleaved by the Cas12a system (Fig. 1a) based on our previous finding (Li et al., 2020). Thrombin binding aptamer (TBA) (Bock et al., 1992; Limongelli et al., 2013), a 15-nt ssDNA (GGTTGGTGTGGTTGG) that binds and inhibits thrombin, was reported to form G4 and has been extensively studied (Jiang et al., 2015; Kovačič et al., 2020). TBA11 (GGTTGGTGTGG) is a truncated form of TBA that forms G3 structure in potassium solution (Limongelli et al., 2013; Wang et al., 2013). To test the above hypothesis, SARS-CoV-2 N-gene was selected as the target and SARS-CoV N-gene as the Control. We labelled the TBA11 sequence with FAM and TAMRA at the two ends and measured the fluorescence resonance energy transfer (FRET). In the Buffer condition (70 mM KCl, 10 mM Tris-HCl, 10 mM $MgCl_2$, pH7.9; no plasmid added), TBA11 demonstrated strong FRET signal (Fig.1a and Fig. S1a), which suggests that it formed a higher-order structure (Li et al. 2012, 2014, 2020bib_Li_et_al_2020bib_Li_et_al_2014bib_Li_et_al_2012). Under the Sample condition (containing the target SARS-CoV-2 N-gene with a sequence complementary to the crRNA), the FRET efficiency dramatically decreased, suggesting the separation of the two fluorophores due to the cleavage. However, the FRET signal in the Control condition (containing SARS-CoV N-gene that does not match with the crRNA) is similar to that of the Buffer condition, revealing no occurrence of cleavage. In addition, we used CD spectroscopy to characterize the cleavage. As shown in Fig. S1b, the Buffer and Control conditions demonstrated similar CD spectra that are highly consistent to that of TBA11 reported in literatures (two positive peaks at 289 nm and 253 nm, and a negative peak at 265 nm) (Jiang et al., 2015; Limongelli et al., 2013; Wang et al., 2013). For the Sample condition, the two positive peaks of the spectrum clearly shifted, suggesting the G3 structure was disrupted.

Furthermore, we used denaturing PAGE to examine the cleavage products under these conditions. Fig. 1c shows that the Buffer and Control conditions have a similar single band, while the Sample condition shows several bands with much lower molecular weights (around 3–6 nt). A Buffer condition without K^+ (the TBA11 oligonucleotide should present as a linear structure) was also tested in the gel and it shows a similar band like the Control. These gel results suggest that TBA11 was cleaved in the Sample condition, while it kept intact in the Control conditions due to the absence of target or no activated Cas12a.

Finally, we applied NMR to verify the trans-cleavage of Cas12a on TBA11-G3. Before the cleavage, the 1D ^1H NMR spectrum (Fig. 1d, left panel) shows the presence of a hydrogen-bonded structure, which is supported by the resonances between 10 and 12 ppm region that is recognized as the characteristic signal of DNA structures with Hoogsteen hydrogen bonds (Limongelli et al., 2013; Wang and Patel, 1993). After the cleavage, the sharp peaks in this region almost disappeared due to the degradation of G3 structure (Fig. 1d, right panel). In addition, the region of aromatic protons (6.5–8.5 ppm, attributed to guanine H8 and thymine H6) (Limongelli et al., 2013) shows significant changes after the cleavage, where the sharper and narrower peaks indicate that some smaller elements were probably produced. In summary, these data collectively corroborate that CRISPR-Cas12a trans-cleaved the TBA11-G3 structure.

3.2. Cleavage kinetics of CRISPR-Cas12a on TBA11-G3

Next, we studied the cleavage kinetics on TBA11 by using time-lapse fluorescence spectroscopy. We did not observe clear fluorescence change before adding the target sequence (data not shown), indicating no trans-cleavage activity, consistent with the previous report (Swarts and Jinek, 2019). After adding the target, the peak value at 518 nm increased gradually over time and achieved the maximum in 20 min (Fig. 2a), suggesting the completion of the trans-cleavage. Fig. 2b shows that the calculated FRET efficiency (Green et al., 2003) decreased ~90% in 5 min, which represents a cleavage rate as fast as cutting ssDNA (Chen et al., 2018). We also studied the cleavage kinetics on TBA-G4. Fig. S2

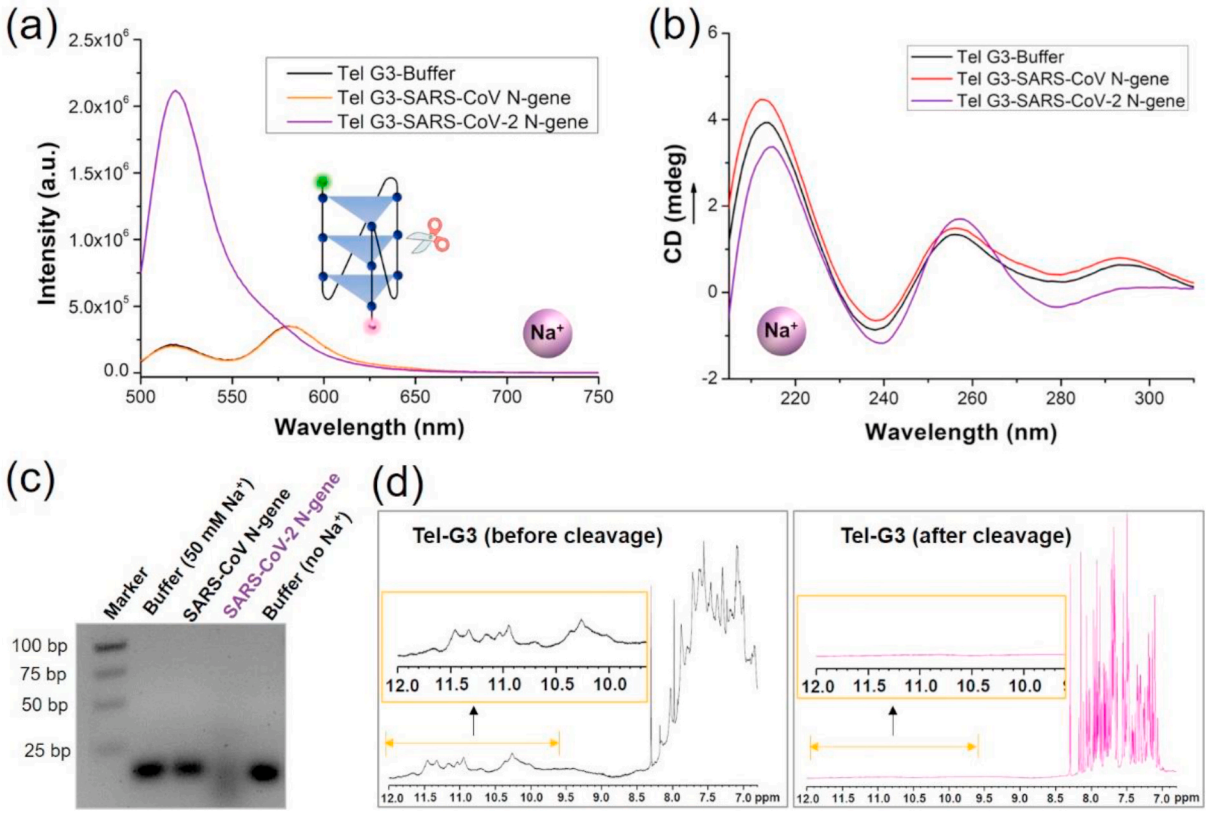

Fig. 3. The trans-cleavage of CRISPR-Cas12a on Na^+ -induced Telomere (Tel) G3 structure. (a-d) Investigation of the trans-cleavage by FRET (a), CD (b), agarose gel electrophoresis (c) and ^1H NMR (d). For lane 2 and lane 5 in (c), no plasmid was added. Sodium concentrations were 50 mM in (a) and (c), and 100 mM in (b) and (d), respectively.

demonstrates that the full cleavage of TBA-G4 (with the same starting concentration as TBA11) required a longer time (~80 min) than TBA11-G3, presumably due to the higher stability of TBA-G4 structure.

Furthermore, we used CD to evaluate the conformational changes of TBA11-G3 during the cleavage. To see the changes more clearly, a higher TBA11 concentration was used. Consistent with Fig. S1c, the CD curves show the time-course shift of the two positive peaks from 253 nm to 289 nm–258 nm and 285 nm, respectively (Fig. 2c). Additionally, we used denaturing PAGE to confirm the cleavage kinetics. The trans-cleavage products at 2.5 min, 5 min, 10 min and 2 h were examined. As shown in Fig. 2d, the trans-cleavage occurred in a very short time and produced some fractions in 2.5 min (lane 2). As cleavage proceeded, more products with smaller molecular weights appeared and increased. The bands in lane 5 show that TBA11-G3 was finally cut into products with 3–6 nt (Fig. 2d), in agreement with Fig. 1c.

3.3. Trans-cleavage on telomere-G3 by Cas12a

Telomeric G-rich sequence of $(TAAGGG)_3TTA$ has been reported to form G3 structure (Tel-G3) in Na^+ solution (Koirala et al., 2012; Li et al., 2013). To test whether the CRISPR-Cas12a system also trans-cleaves other G3 structures besides TBA11-G3, we analyzed the cleavage activity on Tel-G3 by using similar strategies applied to TBA11. As shown in Fig. 3a, the significant difference of fluorescence spectrum between the Sample and Control condition reveals that Tel-G3 was cleaved. The CD spectra of the Controls shown in Fig. 3b are highly consistent to that reported in the literature (Koirala et al., 2012). CD spectrum suggests that the position and magnitude of the original characteristic peaks changed after cleavage. In addition, the gel electrophoresis results further substantiate that the Tel-G3 oligonucleotide was cut into multiple segments with different molecular weights (Fig. 3c). The ^1H NMR spectrum verifies that the G3 structure was degraded after the cleavage, shown by the disappeared resonances in the range of 10–12 ppm and the appearance of sharper and narrower peaks between 6.5 and 8.5 ppm (Fig. 3d). These results suggest that the Na^+-induced Tel-G3 was trans-cleaved by the CRISPR-Cas12a system. Moreover, we confirmed the cleavage of K^+-induced Tel-G3 via the same Cas12a machinery, as evidenced by the fluorescence spectra, CD spectra, and gel electrophoresis results in Fig. S3.

Table 1
Observed cleavage rates (OCRs) of various G4 and G3 structures in the presence of 50 mM Na^+ or 70 mM K^+.

Sequence	Condition	OCR, min^{-1}	R^2
TBA11 (G3)	70 mM K^+	0.350	0.993
TBA15 (G4)	70 mM K^+	0.078	0.983
Telomere-G3	50 mM Na^+	0.223	0.994
	70 mM K^+	0.149	0.997
Telomere-G4	50 mM Na^+	0.182	0.984
	70 mM K^+	0.010	0.996

Lastly, we studied the cleavage kinetics of Na^+- and K^+-induced Tel-G3, and compared with that of Tel-G4 (Fig. S4-5, Table S1). In the presence of Na^+, the cleavage time was about 20 min for Tel-G3 and 30 min for Tel-G4. In the presence of K^+, however, the time it took to fully cut the two structures exhibits significant differences, with about 40 min for Tel-G3 and 800 min for Tel-G4.

3.4. Comparison of Cas12a cleavage rate on G3 and G4

The above results of cleavage kinetics reveal that the trans-cleavage rates of Cas12a on G3 and G4 structures are different and dependent on the ions presented in the buffer. To directly compare the cleavage rates, the kinetics data derived from the time-lapse fluorescence spectra (as

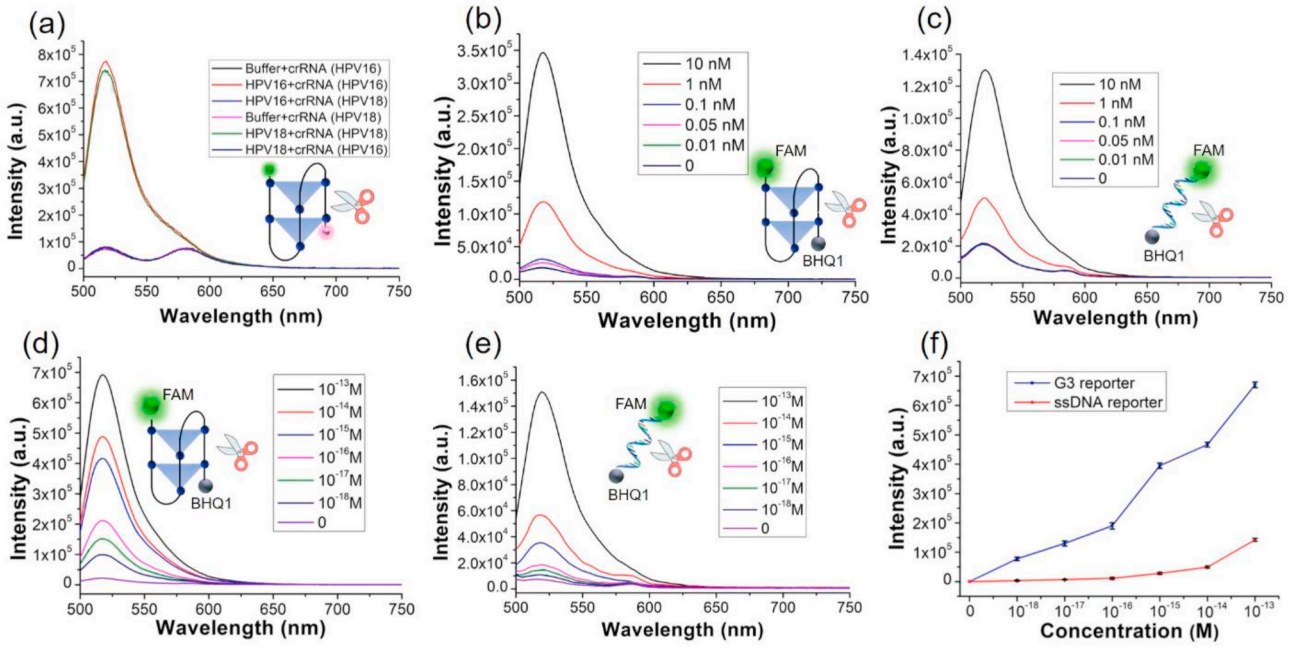

Fig. 4. ***Investigation of the specificity and sensitivity of G-CRISPR.*** *(a) Testing of HPV16 and HPV18 plasmids by using the relevant crRNAs. (b, c) Testing of the unamplified HPV16 plasmid with TBA11-G3 (b) and ssDNA (c) as the reporter. (d, e) Testing of the amplified HPV16 plasmid with TBA11-G3 (d) and ssDNA (e) as the reporter. (f) Dose-response curve of the detection of HPV16 plasmids using the two types of reporters. Error bars represent the standard derivations of three measurements.*

shown in Fig. 2b, Fig. S2b, Fig. S4b, c and Fig. S5b, c) were fit to a single exponential decay curve as summarized in Table 1. These data demonstrate that: first, the observed cleavage rate (OCR) of G3 is higher than that of G4 in the same ion condition; second, the OCR of TBA11-G3 is higher than Tel-G3, and TBA-G4 is higher than Tel-G4 in 70 mM K^+ solution; third, TBA11-G3 is the easiest to be trans-cleaved among these G3 and G4 structures. Previous studies suggest that the stability or melting temperatures (T_m) of G4 and G3 structures are highly associated with the structure type (*i.e.*, G3 or G4) and the ion presented in the buffer (Jiang et al., 2015; Largy et al., 2016; Wlodarczyk et al., 2005). For example, the T_m of TBA and TBA11 in K^+ buffer were reported to be 48.9 °C and 26.4 °C respectively (Jiang et al., 2015); and the observed cleavage rates of the two structures were 0.078 and 0.350 min^{-1} as shown in Table 1. These results indicate that the trans-cleavage rate of Cas12a depends on the stability of G3s and G4s, and the cleavage might involve the unfolding of the high-order structures.

3.5. Establishment of a sensitive biosensing platform "G-CRISPR"

The above results demonstrate that TBA11-G3 is relatively easier to be trans-cleaved than other G3 or G4 structures, which renders it a good candidate as a CRISPR-Cas12a reporter. We thus developed a biosensor, termed G-CRISPR, by coupling TBA11-G3 and CRISPR-Cas12a. We evaluated the performance of G-CRISPR by detecting Human papillomavirus (HPV) DNA. HPV is a DNA virus spread between people through skin-to-skin contact (Mirabello et al., 2017). HPV16 and HPV18 are the two most common subtypes of HPV that could cause cervical cancer among other devastating diseases (Aguirre-Ghiso, 2007; Mirabello et al., 2017). To investigate if G-CRISPR could distinguish the two subtypes, target sequences that varied by six base pairs between the two HPV genotypes were selected in L1-encoding gene of HPV16 and HPV18 (as shown in Supporting Information). For the synthetic targets, the crRNA designed for HPV16 and HPV18 selectively activated Cas12a when the specific targets were present in the test solutions (Fig. 4a). The changes of FRET signals show that our Cas12a-based sensing technology offers high specificity for HPV16 and HPV18 detection. Additionally, the results in Fig. S6 show that G-CRISPR has a good stability in the testing of HPV16 plasmid samples.

For biosensing, detection sensitivity is another critical factor to be considered. This is particularly relevant when disease-related biomarkers or infection virus exhibit low abundance. First, we tested the performance of G-CRISPR for measuring unamplified HPV16 plasmid. FAM and BHQ1 labelled TBA11 (TBA11-FQ) was used as the reporter, and ssDNA-FQ served as the control. As shown in Fig. 4b, the fluorescence intensity at 518 nm increased with the HPV16 concentration changing from 0 to 10 nM. ssDNA-CRISPR could only discriminate Buffer and ~1 nM plasmid (Fig. 4c). G-CRISPR discerned Buffer and 0.05 nM HPV16 plasmid clearly, suggesting better sensitivity than most reported Cas12a-based detection strategies (Ma et al., 2020; van Dongen et al., 2020; Wang et al., 2020a). Moreover, the fluorescence intensity under different conditions (e.g., 0.1 nM and 1 nM plasmid) increased more significantly (~400%) in G-CRISPR than ssDNA-CRISPR (~150%). These data demonstrate that the G3 reporter yields sensitivity ~20 times higher than ssDNA reporter for these unamplified plasmids. The improved sensitivity of G3 reporter could be due to the significant fluorescence change associated with the cleavage-induced high-order structure degradation (Xi et al., 2020), though additional evidence might be required to adequately support this hypothesis.

To further enhance the sensitivity of G-CRISPR, we implemented PCR to amplify the plasmid samples with low concentration ranging from 1×10^{-18} to 1×10^{-13} M. As shown in Fig. 4d and e, the results demonstrate that both the G-CRISPR and ssDNA-CRISPR could differentiate Buffer and the 1×10^{-18} M plasmid sample. However, the fluorescence signals of different samples from the G-CRISPR group vary more distinctly than that of the ssDNA-CRISPR group, which suggests G-CRISPR is better suited for detecting lower concentration samples (e.g., when combined with high-fidelity amplification strategies for trace nucleic acid). The fluorescence signals at 518 nm increased proportionally with the logarithm of plasmid concentrations ranging from 0 to 1×10^{-16} M (Fig. 4f). G-CRISPR and ssDNA-CRISPR yielded a LOD of 0.1 aM (~1 copy/reaction) and 1 aM, respectively. Note that the LOD was calculated based on a 3σ/slope, where σ is the standard deviation of three blank samples (Xiong et al., 2020b). A summary of current Cas12a-based biosensing platforms is included in Table S2, indicating

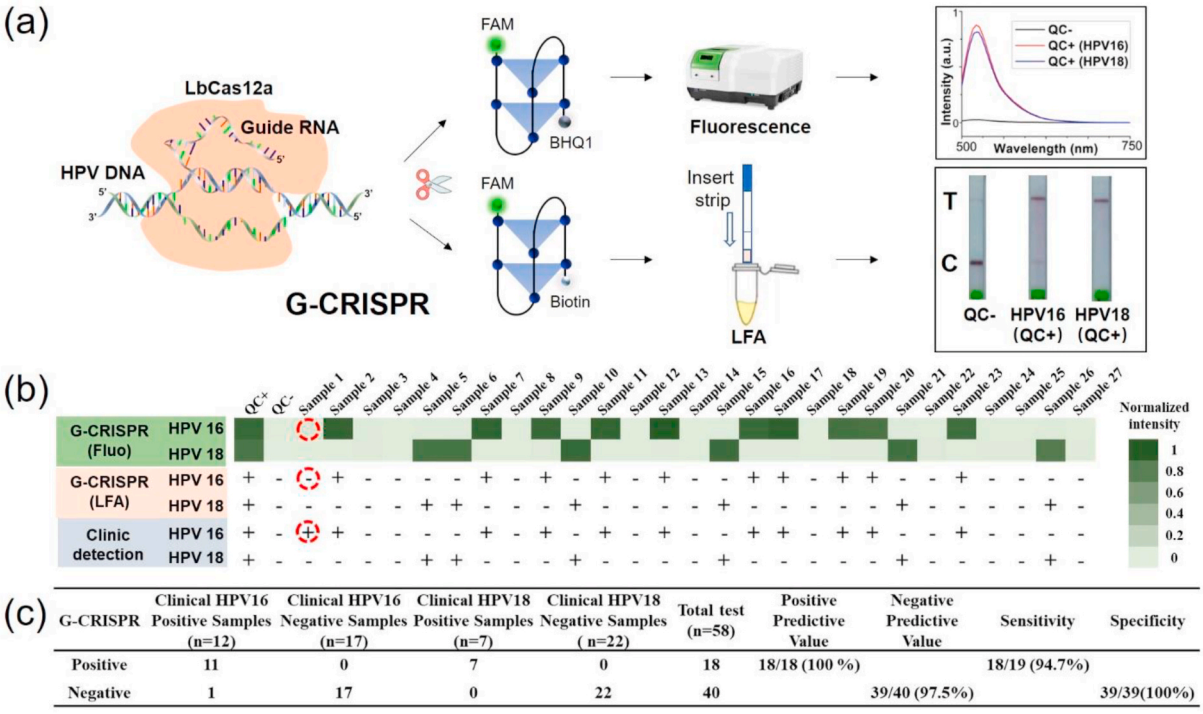

(c)

G-CRISPR	Clinical HPV16 Positive Samples (n=12)	Clinical HPV16 Negative Samples (n=17)	Clinical HPV18 Positive Samples (n=7)	Clinical HPV18 Negative Samples (n=22)	Total test (n=58)	Positive Predictive Value	Negative Predictive Value	Sensitivity	Specificity
Positive	11	0	7	0	18	18/18 (100 %)		18/19 (94.7%)	
Negative	1	17	0	22	40		39/40 (97.5%)		39/39(100%)

Fig. 5. ***Detection of HPV16/18 in patient samples on G-CRISPR.*** *(a) Scheme to show the fluorescence and lateral flow-based G-CRISPR assays. (b) Detection results on G-CRISPR and from the clinic laboratory. The results of the two detections were consistent for all the samples except Sample 1 (HPV16), as shown by the red dotted circle. (c) Positive and negative predictive values, sensitivity, and specificity of G-CRISPR for HPV16/18 detection in the samples.* (For interpretation of the references to colour in this figure legend, the reader is referred to the Web version of this article.)

that our G3-based reporter significantly improves the detection sensitivity.

3.6. HPV16/18 detection in patient samples

To investigate the feasibility of G-CRISPR for analyzing patient samples, we collected crude DNA extractions from 27 human anal swabs analyzed in clinical laboratory for HPV infection (Supporting Information, Table S3). The samples were amplified by PCR and detected with G-CRISPR within 20 min. We used two types of G3 reporters, TbA11-FQ and TBA11-FB (FAM and biotin) to enable the detection based on fluorescence and lateral flow readouts (Fig. 5a). The cleavage assay was carried out on these 27 patient samples and two controls (HPV16+/18+ quality control, and buffer as the negative control). As shown in Fig. 5a, both strategies successfully distinguished the positive and negative controls for the two HPV subtypes. The fluorescence intensity distributed in two groups that were defined as positive and negative samples, respectively (Fig. S7). Fig. S8 showed the instruction for strip result interpretation and Fig. S9 showed the detection results. These two types of readouts yield highly consistent results in agreement with the clinic results for all the samples except Sample 1/HPV16 (Fig. 5b). The fluorescence signal of Sample 1/HPV16 is much lower than other positive samples on G-CRISPR, but still much higher than all the negative samples. Overall, G-CRISPR performed well in testing patient samples, with 100% positive predictive agreement and 97.5% negative predictive agreement (Fig. 5c). Noteworthy, our G-CRISPR platform also exhibits superior sensitivity and specificity with patient samples, *i.e.,* 94.7% and 100%, respectively.

4. Conclusion

We showed for the first time that CRISPR-Cas12a can rapidly transcleave G3 structures and verified this finding by various analytical methods. A novel biosensing platform termed G-CRISPR was developed by integrating Cas12a with unique reporters like TBA11-G3. G-CRISPR offers high stability, specificity and sensitivity for the detection of nucleic acids. Comparing with ssDNA-based systems, G-CRISPR improves the sensitivity up to 20 times and achieves detection sensitivity of 50 pM and 0.1 aM (single copy per reaction) for the unamplified and amplified plasmids, respectively. When tested with 27 clinical HPV samples, G-CRISPR showed high specificity and accuracy, with 100% positive predictive agreement and 97.5% negative predictive agreement. We believe our remarkably accurate, specific, and sensitive G-CRISPR platform holds enormous promise to shift the paradigm of POC diagnostics.

Author contributions

T.L. and R.H. performed the fluorescence, CD, gel and NMR experiments. Y.Y. assisted the NMR experiments. J.X. supervised the clinic sample collection and detection. D.C. collected the clinic samples. Z.X. and J.X. tested the clinical samples. B.L., J.Z., and Y.Y. contributed to the data analysis. Y.L. and M.L. supervised the experimental design and wrote the manuscript. All authors contributed to the revision of this manuscript.

Ethical statement

This study has been carried out in accordance with the Code of Ethics for use of human material and information, and have been approved by the ethics committee of MCHH on Human Research (Approval number: 2020IECXM045).

Declaration of competing interest

The authors declare that they have no known competing financial interests or personal relationships that could have appeared to influence the work reported in this paper.

Acknowledgements

We are grateful to Dr. Zhixiang Tong for his help in the manuscript revision. We gratefully acknowledge the financial supports from National Key R&D Program of China (2018YFA0704000, 2018YFE0202300), National Natural Science Foundation of China (21904139, 21735007, 21991081, 21921004), Chinese Academy of Sciences (Y9Y1041001, YJKYYQ20170026).

Appendix A. Supplementary data

Supplementary data to this article can be found online at https://doi.org/10.1016/j.bios.2021.113292.

References

Abudayyeh, O.O., Gootenberg, J.S., Konermann, S., Joung, J., Slaymaker, I.M., Cox, D.B. T., Shmakov, S., Makarova, K.S., Semenova, E., Minakhin, L., Severinov, K., Regev, A., Lander, E.S., Koonin, E.V., Zhang, F., 2016. C2c2 is a single-component programmable RNA-guided RNA-targeting CRISPR effector. Science 353 (6299), aaf5573.

Aguirre-Ghiso, J.A., 2007. Models, mechanisms and clinical evidence for cancer dormancy. Nat. Rev. Canc. 7 (11), 834–846.

Barrangou, R., Fremaux, C., Deveau, H., Richards, M., Boyaval, P., Moineau, S., Romero, D.A., Horvath, P., 2007. CRISPR provides acquired resistance against viruses in prokaryotes. Science 315, 1709–1712.

Bock, L.C., Griffin, L.C., Latham, J.A., Vermaas, E.H., Toole, J.J., 1992. Selection of single-stranded DNA molecules that bind and inhibit human thrombin. Nature 355 (6360), 564–566.

Broughton, J.P., Deng, X., Yu, G., Fasching, C.L., Servellita, V., Singh, J., Miao, X., Streithorst, J.A., Granados, A., Sotomayor-Gonzalez, A., Zorn, K., Gopez, A., Hsu, E., Gu, W., Miller, S., Pan, C.-Y., Guevara, H., Wadford, D.A., Chen, J.S., Chiu, C.Y., 2020. CRISPR-Cas12-based detection of SARS-CoV-2. Nat. Biotechnol. 38, 870–874.

Cerofolini, L., Amato, J., Giachetti, A., Limongelli, V., Novellino, E., Parrinello, M., Fragai, M., Randazzo, A., Luchinat, C., 2014. G-triplex structure and formation propensity. Nucleic Acids Res. 42 (21), 13393–13404.

Chen, J.S., Ma, E., Harrington, L.B., Da Costa, M., Tian, X., Palefsky, J.M., Doudna, J.A., 2018. CRISPR-Cas12a target binding unleashes indiscriminate single-stranded DNase activity. Science 360 (6387), 436–439.

Dai, Y., Somoza, R.A., Wang, L., Welter, J.F., Li, Y., Caplan, A.I., Liu, C.C., 2019. Exploring the trans-cleavage activity of CRISPR-cas12a (cpf1) for the development of a universal electrochemical biosensor. Angew. Chem. Int. Ed. 58 (48), 17399–17405.

Demkovicova, E., Bauer, L., Krafcikova, P., Tluckova, K., Tothova, P., Halaganova, A., Valusova, E., Viglasky, V., 2017. Telomeric G-quadruplexes: from human to Tetrahymena repeats. J. Nucleic Acids 9170371, 2017.

Ding, X., Yin, K., Li, Z.Y., Lalla, R.V., Ballesteros, E., Sfeir, M.M., Liu, C.C., 2020. Ultrasensitive and visual detection of SARS-CoV-2 using all-in-one dual CRISPR-Cas12a assay. Nat. Commun. 11 (1), 4711.

Doudna, J.A., Charpentier, E., 2014. The new frontier of genome engineering with CRISPR-Cas9. Science 346, 1258096.

Fozouni, P., Son, S., Diaz de Leon Derby, M., Knott, G.J., Gray, C.N., D'Ambrosio, M.V., Zhao, C., Switz, N.A., Kumar, G.R., Stephens, S.I., Boehm, D., Tsou, C.L., Shu, J., Bhuiya, A., Armstrong, M., Harris, A.R., Chen, P.Y., Osterloh, J.M., Meyer-Franke, A., Joehnk, B., Walcott, K., Sil, A., Langelier, C., Pollard, K.S., Crawford, E. D., Puschnik, A.S., Phelps, M., Kistler, A., DeRisi, J.L., Doudna, J.A., Fletcher, D.A., Ott, M., 2020. Amplification-free detection of SARS-CoV-2 with CRISPR-Cas13a and mobile phone microscopy. Cell 184 (2), 323–333 e329.

Gootenberg, J.S., Abudayyeh, O.O., Kellner, M.J., Joung, J., Collins, J.J., Zhang, F., 2018. Multiplexed and portable nucleic acid detection platform with Cas13, Cas12a, and Csm6. Science 360 (6387), 439–444.

Gootenberg, J.S., Abudayyeh, O.O., Lee, J.W., Essletzbichler, P., Dy, A.J., Joung, J., Verdine, V., Donghia, N., Daringer, N.M., Freije, C.A., Myhrvold, C., Bhattacharyya, R.P., Livny, J., Regev, A., Koonin, E.V., Hung, D.T., Sabeti, P.C., Collins, J.J., Zhang, F., 2017. Nucleic acid detection with CRISPR-Cas13a/C2c2. Science 356 (6336), 438–442.

Green, J.J., Ying, L., Klenerman, D., Balasubramanian, S., 2003. Kinetics of unfolding the human telomeric DNA quadruplex using a PNA trap. J. Am. Chem. Soc. 125 (13), 3763–3767.

Harrington, L.B., Burstein, D., Chen, J.S., Paez-Espino, D., Ma, E., Witte, I.P., Cofsky, J.C., Kyrpides, N.C., Banfield, J.F., Doudna, J.A., 2018. Programmed DNA destruction by miniature CRISPR-Cas14 enzymes. Science 362, 839–842.

Ida, J., Chan, S.K., Glökler, J., Lim, Y.Y., Choong, Y.S., Lim, T.S., 2019. G-quadruplexes as an alternative recognition element in disease-related target sensing. Molecules 24 (6), 1079.

Jiang, H.X., Cui, Y., Zhao, T., Fu, H.W., Koirala, D., Punnoose, J.A., Kong, D.M., Mao, H., 2015. Divalent cations and molecular crowding buffers stabilize G-triplex at physiologically relevant temperatures. Sci. Rep. 5, 9255.

Jin, Y.H., Cai, L., Cheng, Z.S., Cheng, H., Deng, T., Fan, Y.P., Fang, C., Huang, D., Huang, L.Q., Huang, Q., Han, Y., Hu, B., Hu, F., Li, B.H., Li, Y.R., Liang, K., Lin, L.K., Luo, L.S., Ma, J., Ma, L.L., Peng, Z.Y., Pan, Y.B., Pan, Z.Y., Ren, X.Q., Sun, H.M., Wang, Y., Wang, Y.Y., Weng, H., Wei, C.J., Wu, D.F., Xia, J., Xiong, Y., Xu, H.B., Yao, X.M., Yuan, Y.F., Ye, T.S., Zhang, X.C., Zhang, Y.W., Zhang, Y.G., Zhang, H.M., Zhao, Y., Zhao, M.J., Zi, H., Zeng, X.T., Wang, Y.Y., Wang, X.H., Management, f.t.Z. H.o.W.U.N.C., Research Team, E.-B.M.C.o.C.I.E., Promotive Association for, M., Health, C., 2020. A rapid advice guideline for the diagnosis and treatment of 2019 novel coronavirus (2019-nCoV) infected pneumonia (standard version). Mil Med Res 7 (1), 4.

Jinek, M., Chylinski, K., Fonfara, I., Hauer, M., Doudna, J.A., Charpentier, E., 2012. A programmable dual-RNA–guided DNA endonuclease in adaptive bacterial immunity. Science 337, 816–821.

Joung, J., Ladha, A., Saito, M., Kim, N.G., Woolley, A.E., Segel, M., Barretto, R.P.J., Ranu, A., Macrae, R.K., Faure, G., Ioannidi, E.I., Krajeski, R.N., Bruneau, R., Huang, M.W., Yu, X.G., Li, J.Z., Walker, B.D., Hung, D.T., Greninger, A.L., Jerome, K. R., Gootenberg, J.S., Abudayyeh, O.O., Zhang, F., 2020. Detection of SARS-CoV-2 with SHERLOCK one-pot testing. N. Engl. J. Med. 383 (15), 1492–1494.

Koirala, D., Mashimo, T., Sannohe, Y., Yu, Z., Mao, H., Sugiyama, H., 2012. Intramolecular folding in three tandem guanine repeats of human telomeric DNA. Chem. Commun. 48 (14), 2006–2008.

Koonin, E.V., Makarova, K.S., Zhang, F., 2017. Diversity, classification and evolution of CRISPR-Cas systems. Curr. Opin. Microbiol. 37, 67–78.

Kovačič, M., Podbevšek, P., Tateishi-Karimata, H., Takahashi, S., Sugimoto, N., Plavec, J., 2020. Thrombin binding aptamer G-quadruplex stabilized by pyrene-modified nucleotides. Nucleic Acids Res. 48 (7), 3975–3986.

Largy, E., Mergny, J.L., Gabelica, V., 2016. Role of alkali metal ions in G-quadruplex nucleic acid structure and stability. In: The Alkali Metal Ions: Their Role for Life. Springer Verlag (Germany), vol. 16, pp. 203–258.

Li, S.-Y., Cheng, Q.-X., Liu, J.-K., Nie, X.-Q., Zhao, G.-P., Wang, J., 2018a. CRISPR-Cas12a has both cis- and trans-cleavage activities on single-stranded DNA. Cell Res. 28 (4), 491–493.

Li, S.Y., Cheng, Q.X., Wang, J.M., Li, X.Y., Zhang, Z.L., Gao, S., Cao, R.B., Zhao, G.P., Wang, J., 2018b. CRISPR-Cas12a-assisted nucleic acid detection. Cell Discovery 4, 20.

Li, W., Hou, X.M., Wang, P.Y., Xi, X.G., Li, M., 2013. Direct measurement of sequential folding pathway and energy landscape of human telomeric G-quadruplex structures. J. Am. Chem. Soc. 135 (17), 6423–6426.

Li, Y., Li, T., Liu, B.F., Hu, R., Zhu, J., He, T., Zhou, X., Li, C., Yang, Y., Liu, M., 2020. CRISPR-Cas12a trans-cleaves DNA G-quadruplexes. Chem. Commun. 56, 12556, 12529.

Li, Y., Liu, C., Feng, X., Xu, Y., Liu, B.F., 2014. Ultrafast microfluidic mixer for tracking the early folding kinetics of human telomere G-quadruplex. Anal. Chem. 86 (9), 4333–4339.

Li, Y., Xu, Y., Feng, X., Liu, B.F., 2012. A rapid microfluidic mixer for high-viscosity fluids to track ultrafast early folding kinetics of G-quadruplex under molecular crowding conditions. Anal. Chem. 84 (21), 9025–9032.

Liang, M.D., Li, Z.L., Wang, W.S., Liu, J.K., Liu, L.S., Zhu, G.L., Karthik, L., Wang, M., Wang, K.F., Wang, Z., Yu, J., Shuai, Y.T., Yu, J.M., Zhang, L., Yang, Z.H., Li, C., Zhang, Q., Shi, T., Zhou, L.M., Xie, F., Dai, H.Q., Liu, X.T., Zhang, J.Y., Liu, G., Zhuo, Y., Zhang, B.C., Liu, C.L., Li, S.S., Xia, X.K., Tong, Y.J., Liu, Y.W., Alterovitz, G., Tan, G.Y., Zhang, L.X., 2019. A CRISPR-Cas12a-derived biosensing platform for the highly sensitive detection of diverse small molecules. Nat. Commun. 10, 3672.

Limongelli, V., De Tito, S., Cerofolini, L., Fragai, M., Pagano, B., Trotta, R., Cosconati, S., Marinelli, L., Novellino, E., Bertini, I., Randazzo, A., Luchinat, C., Parrinello, M., 2013. The G-triplex DNA. Angew Chem. Int. Ed. Engl. 52 (8), 2269–2273.

Ma, P., Meng, Q., Sun, B., Zhao, B., Dang, L., Zhong, M., Liu, S., Xu, H., Mei, H., Liu, J., Chi, T., Yang, G., Liu, M., Huang, X., Wang, X., 2020. MeCas12a, a highly sensitive and specific system for COVID-19 detection. Adv. Sci. 7 (20), 2001300.

Mirabello, L., Yeager, M., Yu, K., Clifford, G.M., Xiao, Y., Zhu, B., Cullen, M., Boland, J.F., Wentzensen, N., Nelson, C.W., Raine-Bennett, T., Chen, Z., Bass, S., Song, L., Yang, Q., Steinberg, M., Burdett, L., Dean, M., Roberson, D., Mitchell, J., Lorey, T., Franceschi, S., Castle, P.E., Walker, J., Zuna, R., Kreimer, A.R., Beachler, D.C., Hildesheim, A., Gonzalez, P., Porras, C., Burk, R.D., Schiffman, M., 2017. HPV16 E7 genetic conservation is critical to carcinogenesis. Cell 170 (6), 11.

Pan, Y., Yang, J., Luan, X., Liu, X., Li, X., Yang, J., Huang, T., Sun, L., Wang, Y., Lin, Y., Song, Y., 2019. Near-infrared upconversion–activated CRISPR-Cas9 system: a remote-controlled gene editing platform. Science Advances 5 (4), eaav7199.

Ramachandran, A., Huyke, D.A., Sharma, E., Sahoo, M.K., Huang, C.H., Banaei, N., Pinsky, B.A., Santiago, J.G., 2020. Electric field-driven microfluidics for rapid CRISPR-based diagnostics and its application to detection of SARS-CoV-2. P Natl Acad Sci USA 117 (47), 29518–29525.

Shao, N., Han, X., Song, Y., Zhang, P., Qin, L., 2019. CRISPR-Cas12a coupled with platinum nanoreporter for visual quantification of SNVs on a volumetric bar-chart chip. Anal. Chem. 91 (19), 12384–12391.

Swarts, D.C., Jinek, M., 2019. Mechanistic insights into the cis- and trans-acting DNase activities of Cas12a. Mol. Cell 73 (3), 589–600 e584.

van Dongen, J.E., Berendsen, J.T.W., Steenbergen, R.D.M., Wolthuis, R.M.F., Eijkel, J.C. T., Segerink, L.I., 2020. Point-of-care CRISPR/Cas nucleic acid detection: recent advances, challenges and opportunities. Biosens. Bioelectron. 166, 112445.

Wang, M., Zhang, R., Li, J., 2020a. CRISPR/cas systems redefine nucleic acid detection: principles and methods. Biosens. Bioelectron. 165, 112430.

Wang, S., Fu, B., Peng, S., Zhang, X., Tian, T., Zhou, X., 2013. The G-triplex DNA could function as a new variety of DNA peroxidase. Chem. Commun. 49 (72), 7920–7922.

Wang, X.S., Xiong, E.H., Tian, T., Cheng, M., Lin, W., Wang, H., Zhang, G.H., Sun, J., Zhou, X.M., 2020b. Clustered regularly interspaced short palindromic repeats/cas9-mediated lateral flow nucleic acid assay. ACS Nano 14 (2), 2497–2508.

Wang, Y., Patel, D.J., 1993. Solution structure of the human telomeric repeat d[AG3 (T2AG3)3] G-tetraplex. Structure 1 (4), 263–282.

Wlodarczyk, A., Grzybowski, P., Patkowski, A., Dobek, A., 2005. Effect of ions on the polymorphism, effective charge, and stability of human telomeric DNA. Photon correlation spectroscopy and circular dichroism studies. J. Phys. Chem. B 109 (8), 3594–3605.

Xi, H., Juhas, M., Zhang, Y., 2020. G-quadruplex based biosensor: a potential tool for SARS-CoV-2 detection. Biosens. Bioelectron. 167, 112494.

Xiong, E., Jiang, L., Tian, T., Hu, M., Yue, H., Huang, M., Lin, W., Jiang, Y., Zhu, D., Zhou, X., 2020a. Simultaneous dual-gene diagnosis of SARS-CoV-2 based on CRISPR/Cas9-Mediated lateral flow assay. Angew. Chem. Int. Ed. 60 (10), 5307–5315.

Xiong, Y., Zhang, J., Yang, Z., Mou, Q., Ma, Y., Xiong, Y., Lu, Y., 2020b. Functional DNA regulated CRISPR-cas12a sensors for point-of-care diagnostics of non-nucleic-acid targets. J. Am. Chem. Soc. 142 (1), 207–213.

Yuan, C., Tian, T., Sun, J., Hu, M., Wang, X., Xiong, E., Cheng, M., Bao, Y., Lin, W., Jiang, J., Yang, C., Chen, Q., Zhang, H., Wang, H., Wang, X., Deng, X., Liao, X., Liu, Y., Wang, Z., Zhang, G., Zhou, X., 2020. Universal and naked-eye gene detection platform based on the clustered regularly interspaced short palindromic repeats/cas12a/13a system. Anal. Chem. 92 (5), 4029–4037.

Zetsche, B., Gootenberg, J.S., Abudayyeh, O.O., Slaymaker, I.M., Makarova, K.S., Essletzbichler, P., Volz, S.E., Joung, J., van der Oost, J., Regev, A., Koonin, E.V., Zhang, F., 2015. Cpf1 is a single RNA-guided endonuclease of a class 2 CRISPR-Cas system. Cell 163 (3), 759–771.

Zhang, F.T., Nie, J., Zhang, D.W., Chen, J.T., Zhou, Y.L., Zhang, X.X., 2014. Methylene blue as a G-quadruplex binding probe for label-free homogeneous electrochemical biosensing. Anal. Chem. 86 (19), 9489–9495.

Zhao, L.L., Cao, T., Zhou, Q.Y., Zhang, X.H., Zhou, Y.L., Yang, L., Zhang, X.X., 2019. The exploration of a new stable G-triplex DNA and its novel function in electrochemical biosensing. Anal. Chem. 91 (16), 10731–10737.